Decay of unstable states in the presence of colored noise and random initial conditions. II. Analog experiments and digital simulations

J. Casademunt, J. I. Jiménez-Aquino,* and J. M. Sancho
Departament d'Estructura i Constituents de la Matèria, Universitat de Barcelona, Diagonal, 647, E-08028 Barcelona, Spain

C. J. Lambert, R. Mannella, P. Martano,† P. V. E. McClintock, and N. G. Stocks
Department of Physics, University of Lancaster, Lancaster, LA1 4YB, United Kingdom
(Received 18 April 1989)

The decay of an unstable state under the influence of external colored noise has been studied by means of analog experiments and digital simulations. For both fixed and random initial conditions, the time evolution of the second moment $\langle x^2(t)\rangle$ of the system variable was determined and then used to evaluate the nonlinear relaxation time. The results obtained are found to be in excellent agreement with the theoretical predictions of the immediately preceding paper [Casademunt, Jiménez-Aquino, and Sancho, Phys. Rev. A **40**, 5905 (1989)].

I. INTRODUCTION

In the immediately preceding paper,[1] hereinafter referred to as paper I, a formalism was developed for the calculation of the nonlinear relaxation time (NLRT) associated with the decay of an unstable state under the influence of external noise. The noise was assumed to be Gaussian with zero mean, and with a correlation

$$\langle \xi(t)\xi(t')\rangle = \frac{D}{\tau}\exp(|t-t'|/\tau) . \tag{1.1}$$

The theory is generally applicable to systems describable by Langevin-like equations; for convenience, these were cast in the form

$$\dot{x} = v(x) + \frac{1}{\epsilon}g(x)\mu , \tag{1.2}$$

where

$$\dot{\mu} = -\frac{1}{\epsilon^2}\mu + \frac{\sqrt{D}}{\epsilon}\eta(t) , \tag{1.3}$$

$\langle \eta(t)\eta(t')\rangle = 2\delta(t-t')$, $\epsilon^2=\tau$, and the noise variable was scaled as $\mu=\epsilon\xi$. The nonlinear relaxation time associated with an average (over realizations of the noise and over initial conditions) of an arbitrary $\phi(x)$, defined as

$$T = \int_0^\infty \frac{\langle\phi(t)\rangle - \langle\phi\rangle_{\rm st}}{\langle\phi\rangle_i - \langle\phi\rangle_{\rm st}}dt , \tag{1.4}$$

was calculated in general for a range of noise colors and intensities and for different types of initial conditions.

In the present paper, we report the outcome of analog and digital experiments undertaken to test the theoretical results, to confirm that they are applicable to real physical systems, and to investigate their range of validity. The investigations were related specifically to the Landau model defined by

$$\dot{x} = ax - bx^3 + \xi(t) , \tag{1.5}$$

where $a,b>0$. As discussed in paper I, this model has an unstable state at $x=0$ and stable states at $x=\pm\sqrt{a/b}$. In the experiments and simulations, the system was initially set either at $x=0$ (fixed initial condition) or, alternatively, it was set in sequential realizations at initial positions with a distribution centered at $x=0$ (random initial conditions); in either case, it was then released, and the time evolution of the second moment $\langle x^2(t)\rangle$ was determined by squaring and ensemble averaging successive $x(t)$ trajectories.

The analog experiments and digital simulations are described in Secs. II and III, respectively; the value of T obtained from them are presented, compared with theory, and discussed in Sec. IV. Section V summarizes the work and draws conclusions.

II. THE ANALOG EXPERIMENT

An electronic circuit model of (1.5) was constructed. It was driven by external noise and the time evolution of its response from given starting conditions was analyzed by means of a digital data processor. The operating principles of such circuits, and the general philosophy and practice of their application to problems in stochastic nonlinear dynamics, have been discussed in detail elsewhere.[2,3] In this section, we describe the design and operation of the particular circuit used for the present work, and we report the results that have been obtained from it.

A. The electronic circuit

The circuit is based on two analog multipliers[4] and a Miller integrator, connected as shown in Fig. 1. In terms of the scaled variables y and t_s (see below) that were used to optimize its performance, the equation describing the operation of the circuit is readily shown to be

$$\tau_i\dot{y} = [V_s y - y^3 - \xi(t_s)] , \tag{2.1}$$

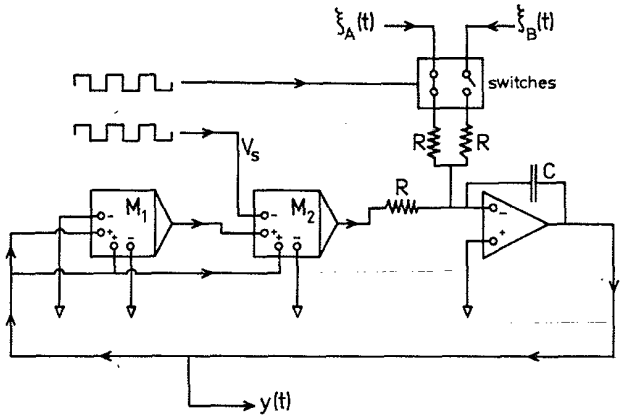

FIG. 1. Block diagram of the analog electronic circuit used to model the time evolution of Eq. (1.5) from specified starting conditions.

where $\tau_i = RC$ is the integrator time constant, $\xi(t_s)$ is exponentially correlated Gaussian noise with correlation function

$$\langle \xi(t_s)\xi(t_s')\rangle = V_{\rm rms}^2 e^{-|t_s - t_s'|/\tau_n} , \tag{2.2}$$

$V_{\rm rms}^2$ is the variance of the noise voltage, and τ_n is its correlation time. The sign and magnitude of the constant voltage V_s can be set externally; in practice, the sign of V_s is alternated periodically, while keeping $|V_s|$ constant, by application of a square wave of amplitude V_s, as shown in the figure. A second square wave of the same frequency and phase is used to operate a pair of solid-state switches through which different forms of external noise $\xi(t_s)$ can be applied to the circuit.

The operation of the circuit for fixed initial conditions was as follows. With V_s negative, so that the corresponding potential has a single minimum at $y=0$, and with no noise applied (switches both open), the system was allowed to settle at $y=0$. The sign of V_s was then suddenly made positive by the next half-cycle of square wave. In terms of the corresponding double-well potential, the system was thereby prepared, such that the representative particle was initially in unstable equilibrium on top of the central maximum at $y=0$. Simultaneously, noise was applied to the circuit (by closing one of the switches) and a sweep of the Nicolet 1080 data processor was triggered. As the system subsequently relaxed towards one or another of the potential minima, its $y(t_s)$ trajectory was digitized (1024 points, 12 bits precision) and the first to fourth moments were computed and added to their ensemble averages. The process was then repeated. The number of blocks in the averages needed to provide acceptable statistical quality depended on the intensity of the applied noise, but was typically in the range 300–3000.

For operation with *random* but *coupled* initial conditions, the sequence of operations was exactly the same, except that one of the noise switches was kept permanently closed. For *random* but *decoupled* initial conditions, both noise generators (see below) were used and the two switches were operated in phase opposition; thus no correlation existed between the noise-producing random fluctuations about the equilibrium position ($y=0$) at the bottom of the single-well potential prior to the transition in the sign of V_s and the noise responsible for the relaxation towards one of the two minima in the double-well potential after the transition.

Particular care was taken to eliminate small dc offsets arising in the multipliers and integrator; the trimming circuitry that was used was of the conventional kind and is not shown in Fig. 1. The scaling factor in the transfer function[4] of the multipliers was reduced below its default value of 10 in order to match the dynamic limits of the circuit more closely to the simulated model. The resultant loss of bandwidth (reduced to 80 kHz) was taken account of, first, by an appropriate choice of integrator time constant (typically $R=10$ kΩ, $C=100$ nF, whence $\tau=RC=10^{-3}$ s) and, second, by an arrangement of the circuit (Fig. 1), such that the noise was injected directly into the summation input of the integrator.

B. Scaling laws for the analog experiment

Although the system to be simulated was the Landau model with unit coefficients

$$\dot{x} = x - x^3 + f(t) , \tag{2.3}$$

it was often necessary in practice to use a value for the amplitude V_s of the square wave in (2.1) that differed from unity. This scaling was in order to ensure that the voltage swings in the circuit were as large as possible in comparison to its own internal noise while, at the same time, ensuring that "clipping" did not occur in any of the components, i.e., that their maximum voltage limits were not exceeded. To match the dynamical behavior of the system to the characteristics of the noise generators, and to enable the measurements to be completed reasonably quickly, the integrator time constant (see above) was chosen to be considerably less than unity. Consequently, the system (2.3) was also being modeled in terms of scaled time.[3] Assuming that the Gaussian random noise $f(t)$ in (2.3) has the correlation function

$$\langle f(t)f(t')\rangle = \frac{D}{\tau} e^{-|t-t'|/\tau} , \tag{2.4}$$

it is straightforward to demonstrate that, if we want to model (2.3) by means of data acquired from (2.1) with an integrator time constant τ_i, the proper scaling relations are

$$D = \langle \xi^2 \rangle \frac{\tau_n}{\tau_i}\frac{1}{V_s^2} = \frac{V_{\rm rms}^2}{V_s^2}\tau , \tag{2.5}$$

$$\tau = \tau_n/\tau_i , \tag{2.6}$$

$$t = t_s V_s/\tau_i , \tag{2.7}$$

$$x = y/V_s^{1/2} . \tag{2.8}$$

C. Noise generators for the analog experiment

For most of the experiments with fixed initial conditions, a standard Wandel and Goltermann model RG2

noise generator was used. For the experiments with random but decoupled initial conditions, however, it was necessary to use a pair of noise generators whose outputs were uncorrelated: a twin-output pseudo-random noise generator was constructed specially for this purpose. It was of the type already described by Martano[5] and used successfully in analog experiments.[6,7] This kind of noise generator is based on the filtering of pseudorandom length sequences of dichotomous pulses to obtain Ornstein-Uhlenbeck noise according to the theorem of Rice.[8] The pulses are generated by a closed-loop-feedback shift-register in which the ex-or feedback function is randomly inverted[5–7] to ex-nor in order to eliminate skewness and thus to obtain a virtually Gaussian distribution.

In the present version of the noise generator, two different stages of the same 18-stage feedback shift register are used as feedback inverters for two quite separate 41-stage shift-registers. In this way, two independent random pulse sequences are obtained which, after filtering, can serve as independent (uncorrelated) noise sources. The clock frequency is 4 MHz. With the filter time constants set to give a frequency cutoff above 40 kHz, the distribution functions of the noise at the outputs were found to be Gaussian to more than ±4 standard deviations. The period of the pseudorandom sequences is about 6.5 days. This time exceeded by a large factor the characteristic times both for an input sweep to the Nicolet data processor (typically 10 ms) and also for the completion of an ensemble average of the statistical moments of several hundred such sweeps (typically 15 min).

D. Analog experimental results

On completion of the ensemble averages of moments for any given set of conditions, the nonlinear relaxation time T defined by (1.4) was computed, usually from the second moment. It was obviously impossible for the upper limit of integration to be ∞ in practice; rather, the data-processor sweep time was adjusted such that $\langle x^2(t)\rangle$ had effectively settled as its final value $\langle x^2\rangle_{st}$ well before the end of the sweep. Some results of these procedures are presented below. In the interests of clarity, the raw values measured in terms of y and t_s, for various values of V_s, have all been scaled to the corresponding values of x and t, so as to be consistent with Eqs. (2.3).

In Fig. 2(a) is shown a typical $x(t)$ input sweep immediately after being digitized by the Nicolet data processor; part (b) of the figure shows the same signal after being squared. A succession of such signals is ensemble averaged to form the moments $\langle x^n(t)\rangle$. Figure 3(a) shows the measured evolution of the second moment under weak noise forcing. The shape of the curve is quite different from that of Fig. 3(b), corresponding to relatively strong noise, where the system starts to rise almost immediately from its initial unstable equilibrium position at $\langle x^2\rangle=0$.

The values of T extracted from data such as those of Fig. 3, for various values of τ and D, and for different initial condition, are presented and discussed below in Sec. IV.

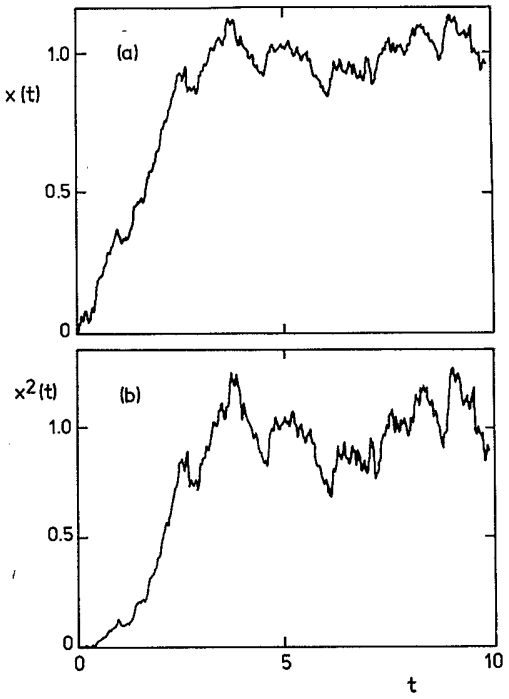

FIG. 2. (a) An example realization of $x(t)$ starting from the initial condition $x=0$ at $t=0$, with $\log_{10}(1/D)=2.00$; $\tau=0.010$. (b) The same example realization as in (a), but after being squared, ready to be added into the memory block in which the second moment $\langle x^2(t)\rangle$ is being ensemble averaged.

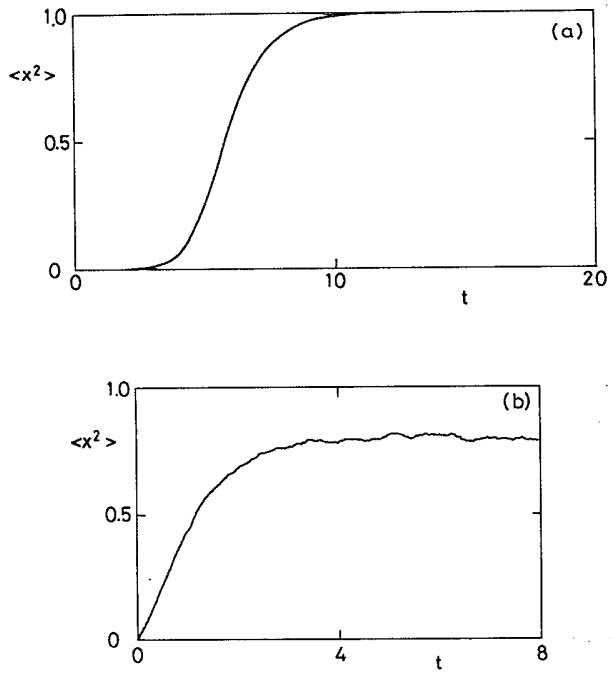

FIG. 3. Measurements of the relaxation of the second moment $\langle x^2(t)\rangle$ from the fixed initial condition $x=0$ at $t=0$ and a noise correlation time $\tau=0.010$, for two different noise intensities D: (a) an average of 300 $x(t)$ trajectories with $\log_{10}(1/D)=4.69$; (b) 3000 trajectories with $\log_{10}(1/D)=0.80$.

III. THE DIGITAL SIMULATION

The digital simulation was performed on an IBM-9375/60 computer using standard algorithms for white and colored noise.[9] Although further removed from being a real physical system, this type of simulation is closer to the ideal theoretical model and has fewer sources of error than the analog experiment. Hence it can be used as a more precise test of the theoretical predictions.

An ensemble of typically 1000 or 2000 realizations is made for each point. The step of integration of the algorithm lies usually between 0.005 and 0.0005. The simulation is carried up to a time typically of the order of $4T_0$, where $T_0 \approx \frac{1}{2}\ln(1/D)$ is an estimate of the time scale of the process. The steady-state value of $\langle x^2 \rangle$ is determined using the data in the time interval $(3T_0, 4T_0)$. The NLRT is obtained from simple numerical integration (trapezoidal rule) of (1.4), from the time-discretized evolution of $\langle x^2 \rangle$ between $t=0$ and $3T_0$.

The simulation of the initial conditions needs a bit more attention. For the case of uncoupled but distributed initial conditions we generate the initial values of x_0 according to the Gaussian distribution (3.7) of paper I, and the values of the noise μ_0 with another independent Gaussian number of variance D. For the case of coupled initial conditions, $\tau \neq 0$, we generate the initial values of x_0 and μ_0 using their joint probability density

$$P_{\rm st}(x_0,\mu_0) \sim \exp\left[-\frac{(1+a_0\tau)}{2D}(\mu_0 - a_0\sqrt{\tau}x_0)^2 - \frac{a_0}{2D}(1+a_0\tau)x_0^2 \right], \tag{3.1}$$

which is the steady solution of the linear model (3.5) of I with colored noise μ. In order to generate the pair of variables (x_0,μ_0) according to the statistics of (3.1) we use two independent Gaussian random numbers of zero mean and unity variance y_1 and y_2, so that

$$x_0 = \frac{\sqrt{D\tau}}{(1+a_0\tau)}y_1 + \frac{\sqrt{D/a_0}}{(1+a_0\tau)}y_2 , \tag{3.2a}$$

$$\mu_0 = \sqrt{D}\,y_1 . \tag{3.2b}$$

For the preparation with the nonlinear model (3.2) of I, the statistics of x_0,μ_0 are not strictly Gaussian. However, for the small intensities of the noise involved, the linear approximation is completely justified since the corrections from the nonlinearities are of higher order than the theoretical predictions.

IV. RESULTS AND COMPARISON WITH THEORY

Given that the theoretical predictions of paper I are asymptotic (small τ, small D), the analog and digital experiments will be useful not only as a confirmation of them but also in order to determine their range of validity. The results we present below correspond to the Landau models (3.2) and (3.4) of paper I with $a=a_0=b=1$.

The concrete predictions that we want to check are Eqs. (3.14), (3.16), (3.17), and (3.19) of paper I. The reference framework will be the white-noise case with fixed initial condition (3.10) of paper I. This result was tested in Refs. 10 and 11 and it is valid for $D \lesssim 0.01$.

Our first result (3.14) of I has been checked for $D=D'$, where D' is the intensity of the noise prior to the "quench" [the change from Eq. (3.2) to Eq. (3.4) of paper I at $t=0$]. The difference predicted in this case is

$$T^D(\tau=0) - T^F(\tau=0) = -\tfrac{1}{2}\ln 2 . \tag{4.1}$$

In Fig. 4, both analog and digital simulations support the predicted shift for all $D \lesssim 0.01$. In this regime, it is clear that the same net effect of speeding the decay is always present, irrespective of how small D is.

Our second prediction (3.16) of paper I establishes that in the case of coupled initial conditions [the "quench" model (3.2) and (3.4) of paper I] the effect of colored noise relative to that of white noise is of higher order than τ. We have checked the importance of these higher-order corrections with digital and analog simulations. In Fig. 5 we see that the relative deviation between both cases is practically zero even for relatively large values of $\tau \approx 1$. The conclusion is that, as far as the decay time is concerned, for a quench experiment the colored-noise case is not essentially different than the white-noise case, so in this kind of problem the white-noise assumption is justified.

The third prediction (3.17) of paper I refers to the NLRT for fixed initial conditions and colored noise. For the model (3.2) the prediction is

$$T_{\rm NL}(\tau) = \frac{1}{2}\left[\ln\frac{1}{D} + \tau \right] + C_{\rm NL} . \tag{4.2}$$

In Fig. 6 we can see the excellent agreement between

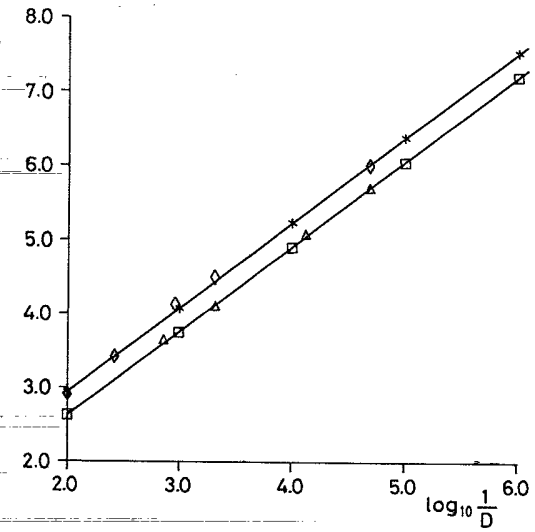

FIG. 4. NLRT vs $\log_{10}(1/D)$ for white noise for fixed and distributed initial conditions ($D'=D$). The straight lines are the theoretical predictions (4.1). Stars ($D'=0$) and squares ($D'=D$) correspond to digital simulation, and rhombics ($D'=0$) and triangles ($D'=D$) to analog simulation.

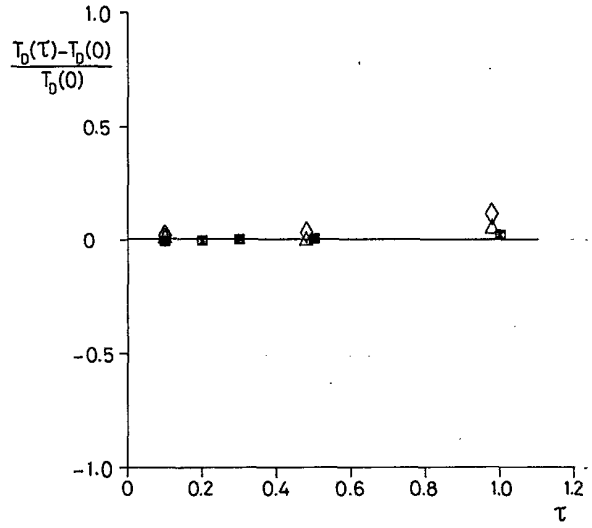

FIG. 5. Relative deviation of the NLRT with coupled initial conditions with respect to the white-noise case vs τ. Stars ($D=10^{-6}$) and squares ($D=10^{-5}$) correspond to digital simulations, and triangles ($D=2.0\times10^{-5}$) and rhombics ($D=4.7\times10^{-4}$) to analog simulations.

(4.2) and both kinds of simulation, covering a wide range of validity for different values of $D \lesssim 0.01$ and $\tau < 1$.

The last prediction (3.19) of paper I refers to the case of distributed initial conditions in the presence of colored noise. For the same distribution of the system variable x, the difference between being and not being coupled to the colored noise in our case, from (3.19) of paper I reads

$$\hat{T}^D(\tau)-T^D(\tau)=\frac{\tau}{2}+O(\tau^2,D,D') \; . \tag{4.3}$$

In Fig. 7(a) we see that this prediction is confirmed in a range of $\tau \lesssim 0.5$.

Finally, we have plotted in Fig. 8 the evolution of the second moment for the linear model (3.3) of paper I and the Landau model (3.2) of paper I for fixed initial conditions and for different intensities of the noise (digital simulation), in order to illustrate the universal law [Eq. (3.10) of paper I]

$$T \approx \frac{1}{a}\left[\frac{1}{2}\ln\left[\frac{R^2 a}{2D}\right]+C\right] \; . \tag{4.4}$$

On the one hand, it is clear that the effect of decreasing

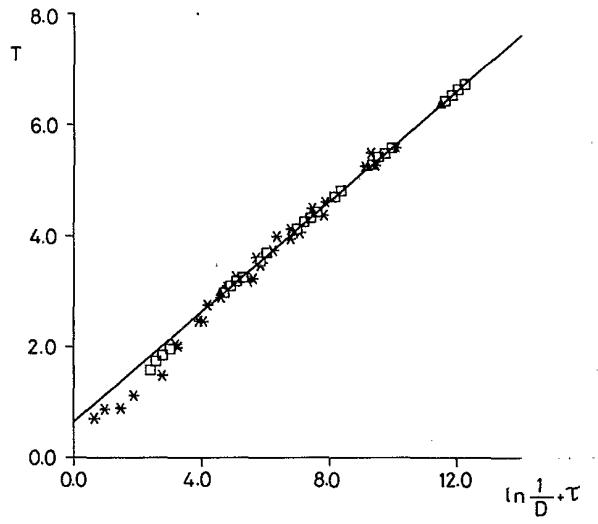

FIG. 6. NLRT with fixed initial condition vs the scaling variable $\ln(1/D)+\tau$. The straight line is the theoretical prediction (4.2). Triangles and squares correspond to digital simulation with white noise and colored noise ($\tau \lesssim 1$), respectively. Stars correspond to analog simulations for colored noise ($\tau \lesssim 1$).

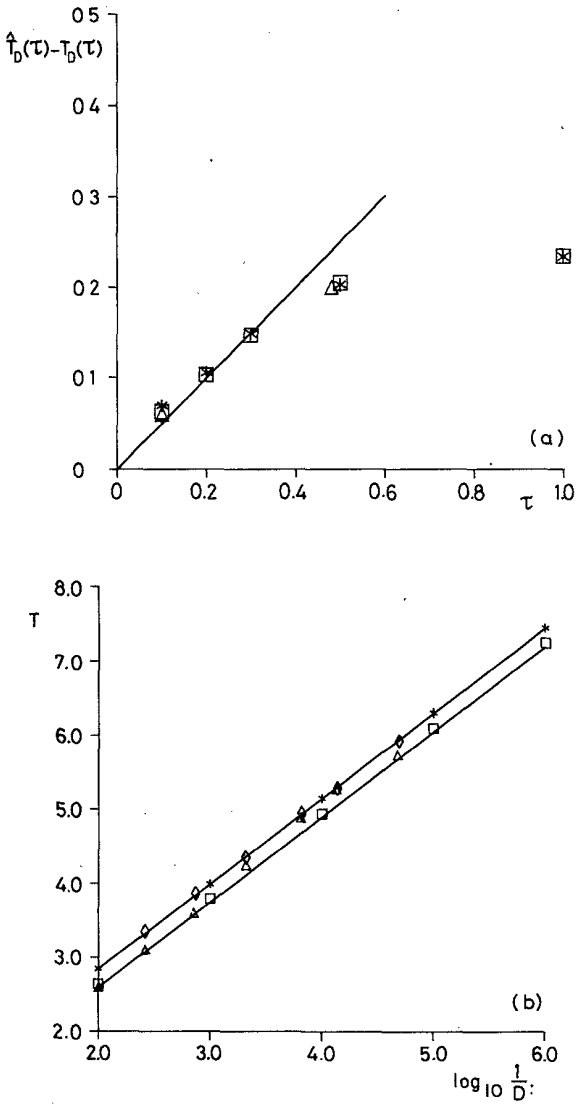

FIG. 7. (a) The difference between the values of T determined for coupled and uncoupled initial conditions, as a function of the noise correlation time τ. The straight line corresponds to the theoretical prediction (4.3). Stars ($D=D'=10^{-6}$) and squares ($D=D'=10^{-5}$) correspond to digital simulation, and the triangles to analog simulation ($D=D'=2.0\times10^{-5}$). (b) The same quantity plotted as a function of $\log_{10}(1/D)$ for $\tau=0.5$. Stars and squares correspond to digital simulations, and rhombics and triangles to analog experiments.

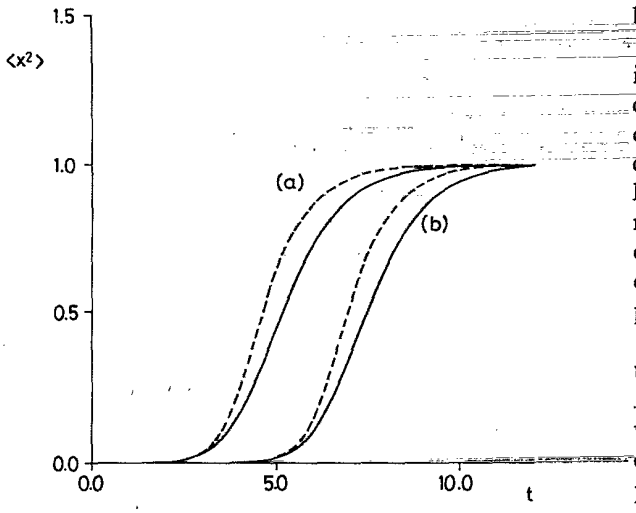

FIG. 8. Digital simulation of the second moment $\langle x^2(t)\rangle$ for fixed initial conditions. The dashes and curves correspond to the model (3.3) of paper I (linear model with reflecting boundaries, $a=R=1$) and the solid ones to the Landau model (1.5) ($a=b=1$). (a) $D=10^{-3}$; (b) $D=10^{-6}$.

the noise intensity is just to shift the entire curve. On the other hand, the details of the shape in the nonlinear and saturation regimes are characteristic of each model and independent of D. Therefore, the constant C contains essentially the information on these last stages of the relaxation. The difference ΔC between the C of a given model and the reference value of the model (3,3) of paper I is essentially the area enclosed between the respective curves. This quantity is a measure of how fast the relaxation is, once the system has escaped from the unstable region.

V. SUMMARY AND CONCLUSIONS

In paper I the study of the decay of unstable states has been presented and theoretical predictions for the NLRT were obtained in different situations. These results were deduced using asymptotic methods and the analog experiments and digital simulation of the present paper have demonstrated their wide range of validity.

The NLRT has provided a global characterization of the decay of unstable states including the final stages of the relaxation. The general picture establishes a universal logarithmic term plus a model-dependent constant which accounts for the nonlinear and saturation regime. This picture is valid for small noise intensities (far-above-threshold condition). For the Landau model this condition turns out to be valid for $bD/a^2 \lesssim 10^{-2}$. In the large noise intensity ($bD/a^2 \gg 1$) domain, the system becomes marginally stable (near threshold).[11]

In these papers, we were interested in the corrections introduced to this general picture by the presence of colored noise and random initial conditions. In all the cases studied, these effects can be taken into account as corrections to the model-dependent constant. Nevertheless, due to the universal character of the responsible mechanisms, which involve only the linear regime, these effects are claimed to be universal and also present in other definitions of characteristic times such as mean-first-passage times.

The prediction for the case of distributed initial conditions with white noise, has been checked in the case $D'=D$ and indirectly in other cases in the calculations involving the Markovian contributions in the colored-noise case. The domain of validity is that of the unstable-state picture we commented on above. It is remarkable that the effect depends on the quotient D/D', so there may be a finite contribution irrespective of how weak the noise is. This could have some relevance in practice in order to determine the actual uncertainty on the initial conditions in "switch-on" problems or the effects of other internal noise sources in a quenching experiment,[12] for instance.

The colored-noise predictions of paper I were done up to first order in τ. The simulations for finite values of τ have shown that the predictions are quite good even for moderate values of τ. The prediction of independence of τ for the coupled case has turned out to be very good for $\tau \approx 1$. This remarkable result means that in a quenched experiment, it is irrelevant whether one has colored or white noise, as far as the decay time is concerned. The prediction for the uncoupled initial conditions, which is the most artificial case, has a shorter domain of validity. The first-order contribution on τ is valid up to $\tau < 0.5$. In the particular case of fixed initial condition with colored noise the predicted law has been shown to be valid for $\tau < 1$.

In general, we have also found that digital simulation mimics the uncoupled case better than the coupled one. The contrary happens in analog experiments which model better the coupled case. This is clear because the coupled case is closer to any real physical situation.

ACKNOWLEDGMENTS

We acknowledge the European Economic Community [Project No. SC1.0043.C (H)], the Dirección General de Investigación Científica y Técnica (Spain) (Project Nos. AE87-0035 and PB87-0014), the British Council, and the Science and Engineering Research Council (U.K.) for the provision of financial support. J. I. J.-A. also acknowledges Consejo National de Ciéncia y Tecnología (Mexico) and Instituto de Cooperación Iberoamericana (Spain) for a grant.

*Present address: Departamento de Física, Universidad Autónoma Metropolitana Iztapalapa, 09340 Mexico Distrito Federal, Mexico.

†Present address: Departamento de Física, Pontifícia Universidade Católica do Rio de Janeiro, Rua Marquês de Sao Vicente 225, Caixa Postal 38071, 22452 Rio de Janeiro, Brazil.

[1] J. Casademunt, J. I. Jimenez-Aquino, and J. M. Sancho, preceding paper, paper I, Phys. Rev. A **40**, 5905 (1989).

[2]L. Fronzoni, in *Noise in Nonlinear Dynamical Systems: Vol. 3, Experiments and Simulations,* edited by F. Moss and P. V. E. McClintock (Cambridge University Press, Cambridge, England, 1989), pp. 222–242.
[3]P. V. E. McClintock and F. Moss, in Ref. 2, pp. 243–274.
[4]Analog Devices type AD534; see specification sheet for details.
[5]P. Martano, laurea thesis, University of Pisa, 1985 (unpublished).
[6]S. Faetti, C. Festa, L. Fronzoni, P. Grigolini, and P. Martano, Phys. Rev. A **30**, 3252 (1984).
[7]S. Faetti, C. Festa, L. Fronzoni, and P. Grigolini, in *Memory Function Approaches to Stochastic Problems in Condensed Matter,* edited by M. W. Evans, P. Grigolini, and G. Pastori-Paravicini (Wiley, New York, 1985), pp. 445–475.
[8]O. Rice, Bell. Syst. Tech. J **23**, 282 (1944).
[9]J. M. Sancho, M. San Miguel, S. L. Katz, and J. D. Gunton, Phys. Rev. A **26**, 1589 (1982).
[10]J. I. Jimenez-Aquino, J. Casademunt, and J. M. Sancho, Phys. Lett. A **133**, 364 (1988).
[11]J. Casademunt, J. I. Jimenez-Aquino, and J. M. Sancho, Physica A **156**, 628 (1989).
[12]M. James, F. Moss, P. Hänggi, and C. Van den Broeck, Phys. Rev. A **38**, 4690 (1988).